J. Fluid Mech. (1979), *vol.* 94, *part* 3, *pp.* 465–475
Printed in Great Britain

The pressure waves produced by the convection of temperature disturbances in high subsonic nozzle flows

By A. W. BLOY
Department of the Mechanics of Fluids, University of Manchester

(Received 15 September 1978 and in revised form 12 March 1979)

The method of characteristics is used to calculate the unsteady one-dimensional flow produced by the convection of a temperature disturbance, contained between two contact surfaces, in high subsonic flow through a nozzle. The results show the development of the pressure disturbances which are associated with the force perturbation needed to accelerate the temperature disturbance at the same rate as the surrounding gas and propagate in both the upstream and downstream directions. Using a simple flow model, expressions for the mean pressure disturbances are derived and shown to be in good agreement with numerical solutions. Other numerical solutions which show the effect of changing the various flow parameters and the nozzle shape are presented. In all of the cases considered, the pressure disturbances caused by a 10 % change in the inlet temperature are significantly large and may be an important part of 'excess' noise.

1. Introduction

Recent work by Hoch & Hawkins (1973) has indicated that part of the 'excess' noise generated internally in a jet engine is linked to the combustion process. Since the combustion process is uneven, it produces pressure disturbances which eventually propagate from the nozzle as sound. This is known as 'direct' combustion noise. Density or temperature fluctuations are also produced and the interaction of these with the flow in the turbine or nozzle gives an 'indirect' noise mechanism.

The nozzle flow problem has been considered by Bohn (1977) and by Marble & Candel (1977) who used a linear analysis of the one-dimensional flow equations with periodic disturbances. Marble & Candel obtained expressions for the pressure disturbances in the case of a 'compact nozzle', i.e. the case where the wavelengths are much longer than the nozzle. For a nozzle of finite length, Bohn as well as Marble & Candel assumed a linear variation of velocity through the nozzle. Ffowcs Williams & Howe (1975) considered the low subsonic convection of a 'slug' of different density fluid through a nozzle with the slug completely filling the nozzle. It was shown that the pressure fluctuations depend on the presence of a mean flow pressure gradient and are associated with a fluctuation in thrust. Howe (1975) reformulated the theory of aerodynamic sound and considered the noise generation due to density 'spots' accelerating in low subsonic flow.

Whitfield & Howe (1976) have produced experimental results, obtained by injecting bubbles into a water jet, which indicate that reduced sound levels can be achieved by reducing the maximum pressure gradient in the nozzle.

0022-1120/79/4325-7660 $02.00

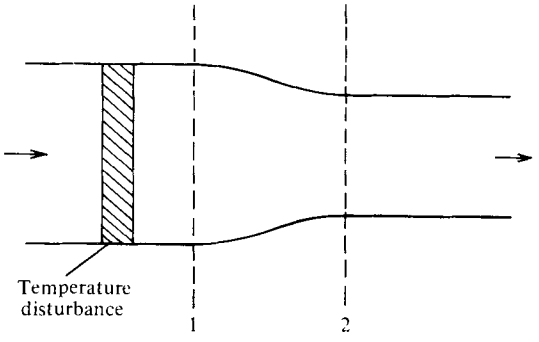

FIGURE 1. Initial steady flow with temperature disturbance.

The flow model used in this paper assumes that a single temperature disturbance, contained between two contact surfaces, is convected through a contraction in a duct as shown in figure 1.

Pressure pulses are produced as the temperature disturbance passes through the contraction and the one-dimensional, unsteady flow is analysed by the method of characteristics. This approach illustrates the development of the pressure pulses and gives an insight into the sound generation mechanism. Flows where the scale of the temperature disturbance is smaller than that of the contraction and of the same order as that of the contraction are considered.

2. Calculation method

The calculations are based on a characteristics network and are initiated from the time at which the first contact surface arrives at the area change. A step-by-step procedure is used to calculate the conditions along the C^+ and C^- characteristic lines and the contact surfaces. The relevant one-dimensional, unsteady flow equations along the characteristic C^+ and C^- directions are

$$dp \pm \rho a\, du + \frac{\rho a^2 u}{A}\frac{dA}{dx}\, dt = 0 \quad \text{on} \quad \frac{dx}{dt} = u \pm a. \tag{1}$$

Along the particle paths

$$dp - a^2 d\rho = 0 \quad \text{on} \quad \frac{dx}{dt} = u. \tag{2}$$

The thermal equation of state is

$$p = \rho RT. \tag{3}$$

p, ρ and T are the pressure, density and temperature, R the gas constant, u the flow speed, a the speed of sound, A the cross-sectional area, x the distance measured from the entrance of the contraction and t the time, taken from the arrival of the first contact surface at the contraction.

These equations are written in a non-dimensional form which is based on the length of the contraction L and the steady flow conditions upstream of the contraction. The flow equations, in the non-dimensional form, are then used to calculate the unsteady flow given the area distribution, the steady flow Mach number downstream of the contraction M_2 and the initial properties of the temperature disturbance, which are its

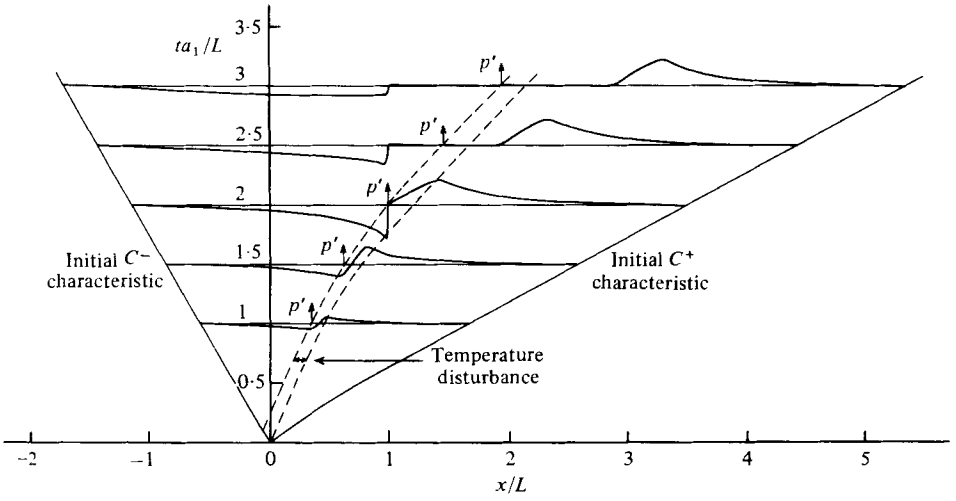

FIGURE 2. Convection of a temperature disturbance through a contraction and the development of the pressure disturbances; $M_2 = 1{\cdot}0$, $A_1/A_2 = 1{\cdot}5$, $\Delta T_1/T_1 = 0{\cdot}1$, $l_1/L = 0{\cdot}1$.

length l_1 and the temperature change ΔT_1 or the density change $\Delta\rho_1$ due to the disturbance. The specific heat ratio γ is taken as $\frac{7}{5}$ and the subscripts 1 and 2 refer to the flow conditions upstream and downstream of the contraction.

The characteristics network is constructed as a series of layers. Each layer starts at the first contact surface and proceeds along the C^+ and C^- characteristics. Linear interpolation along the C^- characteristic is required for the calculation of the contact surface points and the usual methods of iteration, discussed by Sedney (1970), are used for high accuracy. An analytical expression is used to specify the area change.

A numerical problem was encountered in the high subsonic flow region where the Mach number gradient dM/dx was relatively large. In this region, the C^- characteristics tended to diverge rapidly so that the step sizes along the C^+ characteristics became excessive for good accuracy. To overcome this problem a variable step size was used along the initial C^+ characteristic so that small steps were taken in the region where the Mach number gradients were large. The determination of the initial step size was based on the analysis given in the appendix, with suitable values chosen for the time interval over which the calculations were made and for the step size along the final C^+ characteristic. Although the analysis was derived for sonic flow, the expression for the step size was applied to the flow region where the Mach number was between 0·7 and 1·0. A constant step size was taken along the initial C^- characteristic. The value of this step size was that determined by the initial mesh constructed at the first contact surface. A continuous check was made in order to ensure that characteristic lines of the same family did not cross, i.e. to ensure that a shock did not form. This was the case for all the flows considered.

The accuracy of the calculations was checked by comparing the results obtained using different step sizes and, in addition, the conservation of mass and energy within a control volume, which contained the temperature disturbance and the pressure waves, was tested. These checks indicated that satisfactory accuracy was achieved.

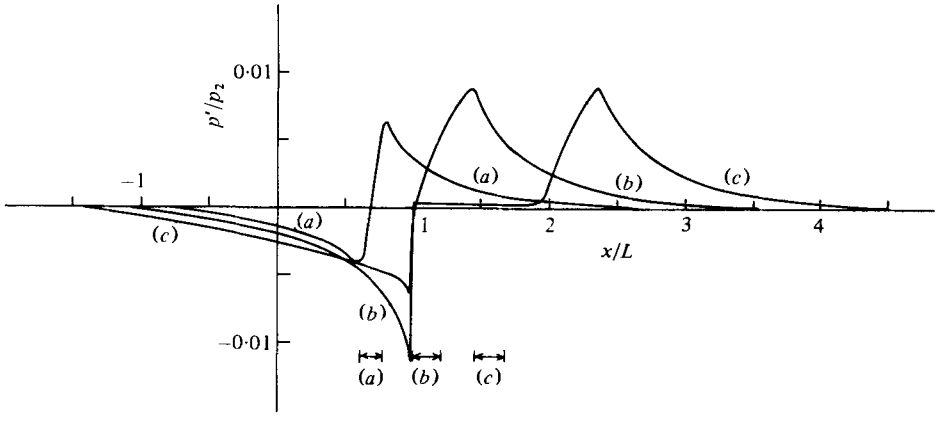

FIGURE 3. Pressure disturbances; $M_2 = 1{\cdot}0, A_1/A_2 = 1{\cdot}5, \Delta T_1/T_1 = 0{\cdot}1, l_1/L = 0{\cdot}1$. (a) $ta_1/L = 1{\cdot}5$. (b) $ta_1/L = 2{\cdot}0$. (c) $ta_1/L = 2{\cdot}5$. $|\leftrightarrow|$, position of temperature disturbance.

3. High subsonic nozzle flow

Calculations were made in order to determine the pressure disturbances produced by the convection of a temperature disturbance through a contraction at high subsonic exit conditions. Figure 2 illustrates the development of the pressure waves for

$$M_2 = 1{\cdot}0, \quad \Delta T_1/T_1 = 0{\cdot}1, \quad l_1/L = 0{\cdot}1$$

and a contraction area ratio $A_1/A_2 = 1{\cdot}5$; p' is the pressure disturbance. A contraction with a smooth inlet and outlet was specified with a profile given by

$$\frac{A}{A_1} = \frac{A_1+A_2}{2A_1} + \frac{A_1-A_2}{2A_1}\cos\left(\frac{\pi x}{L}\right). \tag{4}$$

An initial step size at the origin, $\delta x/L = 0{\cdot}01$, was taken along the first C^+ characteristic.

From the figure, it can be seen that pressure disturbances build up as the temperature disturbance is convected through the contraction. The first contact surface generates compression and expansion waves which propagate downstream and upstream respectively and, for a single contact surface, the flow in the contraction would settle to new steady conditions. However, the passage of the second contact surface through the contraction produces pressure disturbances of the opposite sign, which tend to cancel out the first pressure disturbances. The degree of cancellation depends on the distance between the contact surfaces, the nozzle geometry and the flow conditions. Two resultant waves are formed which eventually propagate away from the temperature disturbance. It appears that the passage of the temperature disturbance essentially involves an expansion of the temperature disturbance which is at the same rate as the steady flow expansion, i.e. there is no differential volume change between the temperature disturbance and the surrounding gas. The sound generation is then associated with the force perturbation required to accelerate the temperature disturbance at the same rate as the surrounding gas. This effect is shown clearly in figure 2 and is equivalent to a dipole source. Furthermore, the wavelengths of the pressure disturbances are determined by the wave speed and a time difference which can be

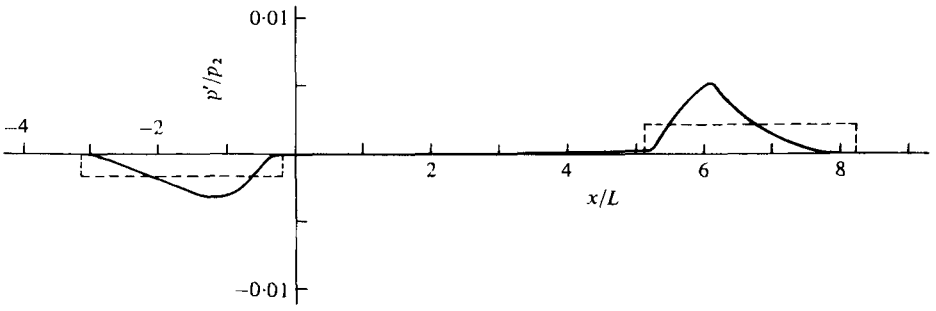

FIGURE 4. Pressure disturbances; $M_2 = 0{\cdot}7$, $A_1/A_2 = 1{\cdot}5$, $\Delta T_1/T_1 = 0{\cdot}1$, $l_1/L = 0{\cdot}2$, $ta_1/L = 5{\cdot}1$. ---, mean pressure disturbances and wavelengths given by equations (13) and (14).

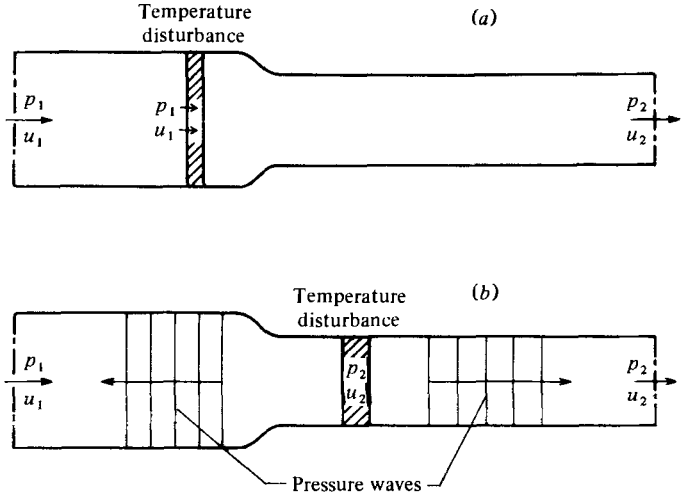

FIGURE 5. Unsteady flow model.

found from the x, t diagram. For the wave which propagates downstream of the contraction, the relevant time is the difference between the transit times through the contraction of the temperature disturbance and a pressure disturbance which propagates along the initial C^+ characteristic. Ffowcs Williams & Howe (1975) have made similar observations on the sound generation mechanism and frequency.

Figure 3 shows the pressure distributions at $ta_1/L = 1{\cdot}5$, $2{\cdot}0$ and $2{\cdot}5$ drawn to scale and it can be seen that the peak values are approximately 1 % of the downstream pressure p_2. The steep pressure gradients which occur near the exit of the contraction are associated with the low wave speed in the upstream direction. It can also be seen from figures 2 and 3 that the flow velocity and pressure in the region between the two waves at $ta_1/L = 2{\cdot}5$ and $3{\cdot}0$ are practically the same as those in the initial steady flow. This feature is further illustrated in figure 4 which presents the calculated pressure disturbances at a lower flow speed and at a time when the two pressure waves are travelling within the constant area ducts. The dashed lines give the rectangular pressure pulses obtained from the following analysis. Energy and mass balances can be set up using the flow model illustrated in figures 5 (*a*) and 5 (*b*), where the pressure and velocity within the temperature disturbance are assumed to be the same as those in the

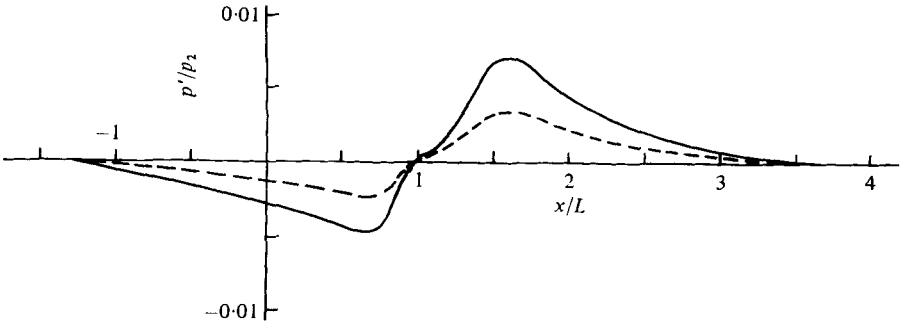

FIGURE 6. Effect of changing disturbance density; $M_2 = 0{\cdot}7$, $A_1/A_2 = 1{\cdot}5$, $l_1/L = 0{\cdot}1$. ---, $\Delta\rho_1/\rho_1 = -0{\cdot}1$. ——, $\Delta\rho_1/\rho_1 = -0{\cdot}2$.

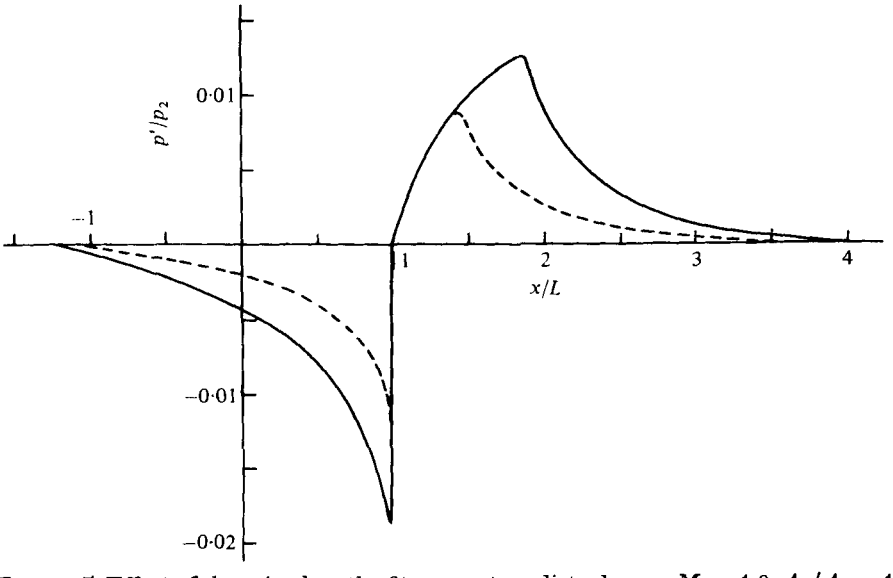

FIGURE 7. Effect of changing length of temperature disturbance; $M_2 = 1{\cdot}0$, $A_1/A_2 = 1{\cdot}5$, $\Delta T_1/T_1 = 0{\cdot}1$. ---, $l_1/L = 0{\cdot}1$; ——, $l_1/L = 0{\cdot}2$.

steady flow case. Since the flow through the end boundaries of the control volume remains steady, it follows that the flow energy and mass within the control volume are conserved, i.e.

$$\int_V \rho E \, dV = \text{constant} \tag{5}$$

and

$$\int_V \rho \, dV = \text{constant}, \tag{6}$$

where V refers to the control volume and E is the sum of the specific internal and kinetic energies. E can be written as

$$E = \frac{1}{(\gamma-1)}\frac{p}{\rho} + \tfrac{1}{2}u^2. \tag{7}$$

Hence, using Δ to indicate the change in conditions due to the temperature disturbance,

$$\Delta(\rho E)_{1,2} = (\tfrac{1}{2}u^2\Delta\rho)_{1,2}. \tag{8}$$

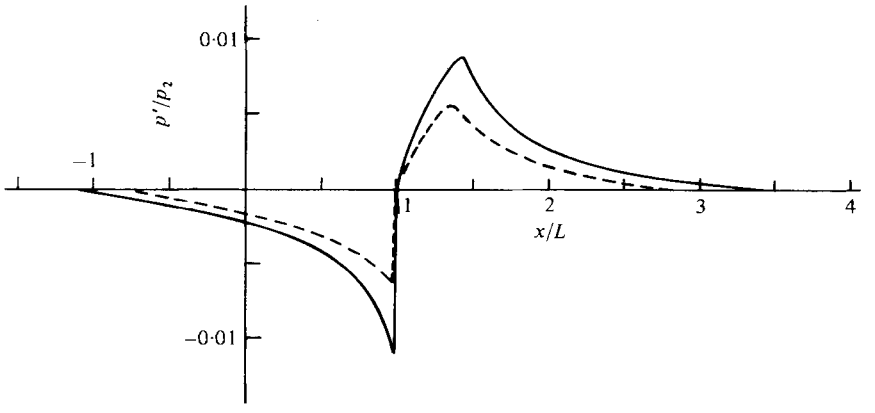

FIGURE 8. Effect of changing contraction area ratio; $M_2 = 1{\cdot}0$, $\Delta T_1/T_1 = 0{\cdot}1$, $l_1/L = 0{\cdot}1$. ---, $A_1/A_2 = 1{\cdot}25$; ——, $A_1/A_2 = 1{\cdot}5$.

For a plane wave travelling in a constant-area duct, acoustic theory gives the following relations

$$(\rho E)' \doteq \left[\frac{1}{(\gamma-1)}\frac{a_0^2}{a^2} \pm M\right] p' \tag{9}$$

and

$$p' = a^2\rho', \tag{10}$$

where the primed terms are the disturbances produced by the pressure waves and subscript 0 refers to the stagnation conditions. Referring to figures 5(*a*) and 5(*b*), the energy balance can be written as

$$[A\lambda\overline{(\rho E)'}]_1 + [A\lambda\overline{(\rho E)'}]_2 + [Al\Delta(\rho E)]_2 = [Al\Delta(\rho E)]_1, \tag{11}$$

where the overbar indicates a mean quantity, λ is the wavelength and l is the length of the temperature disturbance.

For a mass balance within the pressure waves and the temperature disturbance

$$(A\lambda\overline{\rho'})_1 + (A\lambda\overline{\rho'})_2 = (Al\Delta\rho)_1 - (Al\Delta\rho)_2 = 0, \tag{12}$$

λ_1 and λ_2 are approximately given by

$$\lambda_{1,2} = (a \mp u)_{1,2}\left[\frac{l_{1,2}}{u_{1,2}} + \int_0^L \frac{dx}{u} \pm \int_0^L \frac{dx}{a \mp u}\right]. \tag{13}$$

Using equations (8) to (12), one can evaluate the mean pressure disturbances upstream and downstream of the contraction. The results are given by

$$\left(\frac{\overline{p'}}{p}\right)_{1,2} = \pm\gamma\left(\frac{l}{\lambda}\frac{\Delta\rho}{\rho}\right)_{1,2}\frac{\frac{1}{2}(M_2 - M_1)}{1 + \frac{1}{2}(\gamma-1)M_1M_2}. \tag{14}$$

Equation (14) describes the effects of the ratio of the length of the temperature disturbance to the wavelength, the fractional density change and the steady flow conditions upstream and downstream of the contraction. The form of the pressure pulses is determined by the shape of the contraction.

Numerical solutions showing the effect of changing the temperature disturbance and the steady flow conditions are given in figures 6 to 9. These figures show the pressure waves which exist when the temperature disturbance is at the downstream end of

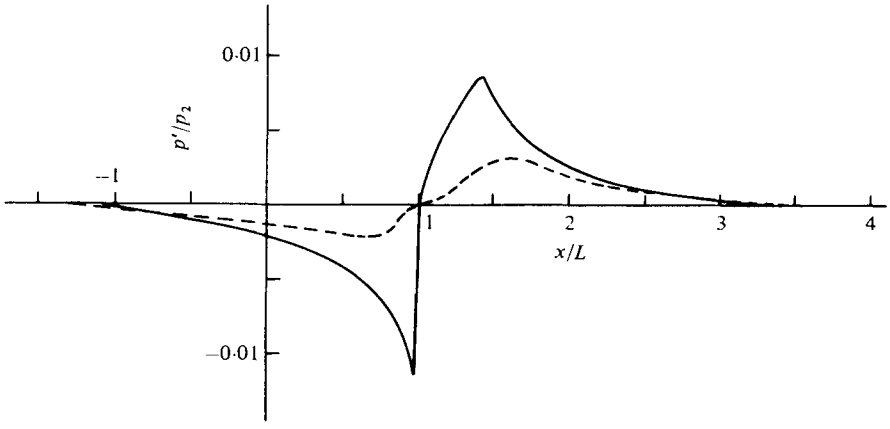

FIGURE 9. Effect of changing downstream Mach number; $A_1/A_2 = 1{\cdot}5$, $\Delta T_1/T_1 = 0{\cdot}1$, $l_1/L = 0{\cdot}1$. ---, $M_2 = 0{\cdot}7$. ——, $M_2 = 1{\cdot}0$.

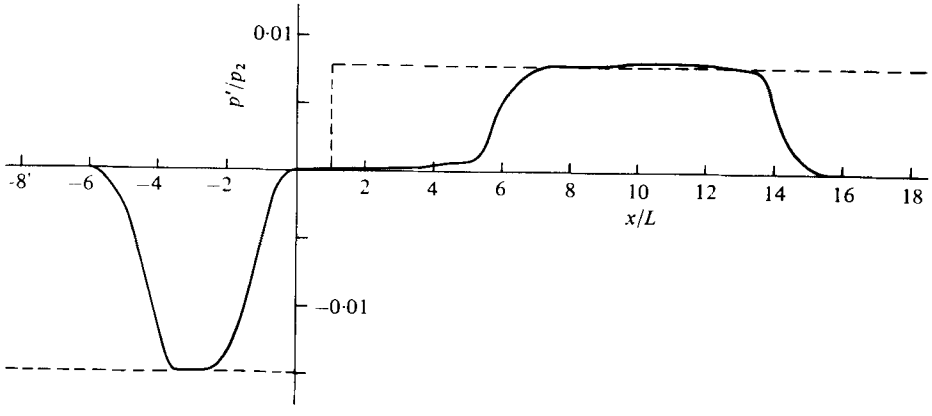

FIGURE 10. Effect of temperature disturbance which fills the contraction; $M_2 = 0{\cdot}7$, $A_1/A_2 = 1{\cdot}5$, $\Delta T_1/T_1 = 0{\cdot}1$, $l_1/L = 2{\cdot}0$, $ta_1/L = 9{\cdot}7$. ---, pressure disturbances given by equation (16) for a compact nozzle.

the contraction with the second contact surface at $x/L = 1{\cdot}0$. In all of these cases, the smooth contraction shape, defined by equation (4), was used, while the steady flow conditions upstream and downstream of the contraction were defined by the area ratio A_1/A_2 and the downstream flow Mach number M_2. The results are consistent with the mean effects given by equation (14).

Additional calculations have indicated that the peak pressure disturbances increase to a plateau value as the temperature disturbance completely fills the contraction as shown by the results given in figure 10 for $M_2 = 0{\cdot}7$, $\Delta T_1/T_1 = 0{\cdot}1$, $l_1/L = 2{\cdot}0$ and $A_1/A_2 = 1{\cdot}5$. The peak pressure disturbances correspond closely to the results derived for a compact nozzle. This is the case where the nozzle length is small in comparison with the temperature disturbance. For the compact nozzle

$$\lambda_{1,2} = (a \mp u)_{1,2} \left(\frac{l}{u}\right)_{1,2},$$

i.e.

$$\left(\frac{l}{\lambda}\right)_{1,2} = \frac{M_{1,2}}{1 \mp M_{1,2}}. \tag{15}$$

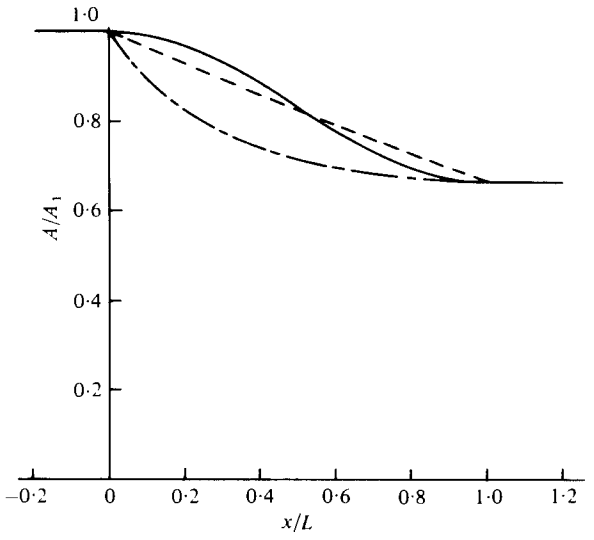

FIGURE 11. Contraction shapes; $A_1/A_2 = 1{\cdot}5$. ---, conical; ———, bellmouth; ——, smooth.

Equation (14) then becomes

$$\left(\frac{p'}{p}\right)_{1,2} = \pm\frac{\gamma M_{1,2}}{1 \mp M_{1,2}}\left(\frac{\Delta\rho}{\rho}\right)_{1,2}\frac{\frac{1}{2}(M_2 - M_1)}{1+\frac{1}{2}(\gamma-1)M_1 M_2}, \tag{16}$$

where $\Delta\rho/\rho$ is approximately equal to $-\Delta T/T$ and has the same value upstream and downstream of the contraction. The expressions given by equation (16) are then in exact agreement with the results of Marble & Candel (1977) for a compact subcritical nozzle.

Three contraction shapes, shown in figure 11, were chosen to show the remaining effect, that of changing the shape of the contraction. These included the smooth contraction shape, a conical contraction and a bellmouth contraction which produced a constant acceleration of the steady flow. Since the conical contraction produces an infinite Mach number gradient at sonic conditions, which would lead to the numerical problem described in §2, the calculations were restricted to a downstream Mach number $M_2 = 0{\cdot}95$. The area ratio A_1/A_2 was taken as 1·5. The results, shown in figure 12, indicate similar distributions of the pressure disturbances for the smooth and conical contractions, apart from the spike produced by the conical contraction near $x/L = 1{\cdot}0$. The other significant feature is that the bellmouth contraction produces lower peak pressure disturbances.

From the present results, it can be inferred that high levels of sound pressure are produced in a high speed jet by this sound mechanism. Consider the following flow conditions which relate to those in the tailpipe of a jet engine. The temperature fluctuation in the duct $\Delta T_1/T_1$ is taken as 0·1; the nozzle area ratio A_1/A_2 is 1·5; the ratio of the initial length of the temperature disturbance l_1 to the nozzle length L is 0·2 and, downstream of the nozzle, the flow is sonic with the static pressure $p_2 = 1$ atm. Then, using the results shown in figure 7, the peak downstream sound pressure level is 156 dB.

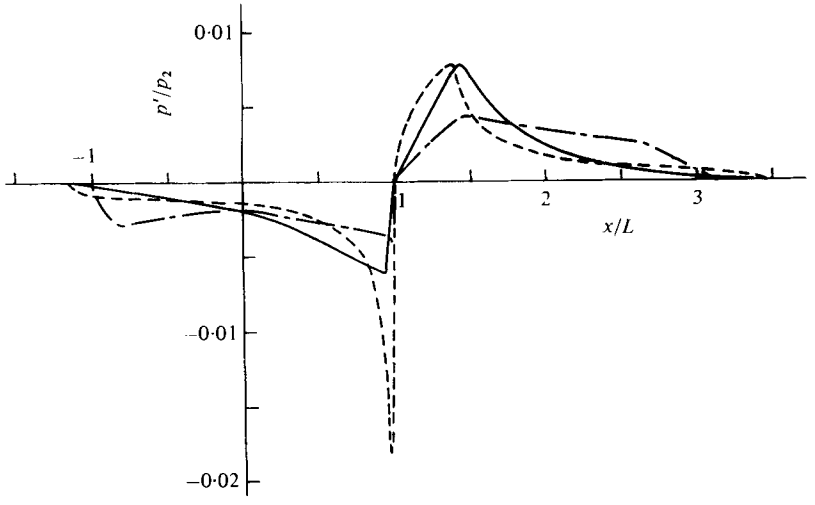

FIGURE 12. Effect of changing contraction shape; $M_2 = 0{\cdot}95$, $A_1/A_2 = 1{\cdot}5$, $\Delta T_1/T_1 = 0{\cdot}1$, $l_1/L = 0{\cdot}1$. ---, conical; — — —, bellmouth; ——, smooth.

4. Conclusions

The development of the pressure disturbances produced by the high subsonic convection of a temperature disturbance through a contraction in a duct is illustrated. Two waves are produced which propagate in the upstream and downstream directions and these waves are associated with a force perturbation which acts on the temperature disturbance as it passes through the contraction. The mean pressure disturbances are accurately predicted from the analysis of a simple flow model which indicates that the pressure disturbances are proportional to the fractional density change due to the temperature disturbance times l/λ, where l and λ are the lengths of the temperature disturbance and the pressure wave respectively.

Other calculations have been made which indicate the effect of changing the various flow conditions and the contraction shape. Of the contraction shapes investigated, a bellmouth contraction was found to produce the lowest peak pressure disturbances.

The author thanks Professor N. H. Johannesen for suggesting this study and for his helpful discussions.

Appendix. Calculation of the initial step size

Consider the points 1, 2, 3, 4 of the characteristics mesh shown in figure 13. The analysis assumes that the flow is steady and that sonic flow conditions exist along the line 2–4. The speed of sound a and the Mach number gradient dM/dx are taken as constant within the mesh. Along the C^- characteristic line 1–3,

$$dx/dt = u - a = a(M-1). \tag{A 1}$$

Since dM/dx is assumed constant,

$$M = M_{2-4} + (x - x_{2-4})\, dM/dx, \tag{A 2}$$

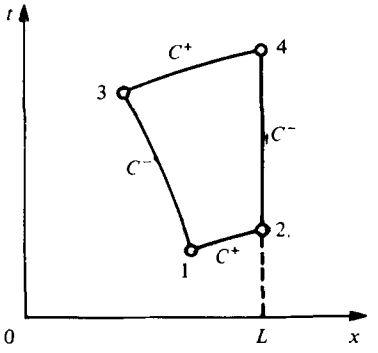

FIGURE 13. Steady flow characteristics mesh for sonic flow at $x = L$.

where $M_{2-4} = 1{\cdot}0$. Substituting in equation (A 1) gives

$$dx/dt = a(x - x_{2-4})\,dM/dx. \tag{A 3}$$

Integrating from 1 to 3 gives

$$\int_{x_1}^{x_3} \frac{dx}{(x - x_{2-4})} = a\frac{dM}{dx}\int_{t_1}^{t_3} dt,$$

i.e.

$$\ln\left(\frac{x_3 - x_4}{x_1 - x_2}\right) = a\frac{dM}{dx}(t_3 - t_1).$$

Hence

$$x_2 - x_1 = (x_4 - x_3)\exp\left[-a\frac{dM}{dx}(t_3 - t_1)\right]. \tag{A 4}$$

The above expression relates the step size $(x_2 - x_1)$ along the initial C^+ characteristic to the step size $(x_4 - x_3)$ along the final C^+ characteristic.

REFERENCES

BOHN, M. S. 1977 Response of a subsonic nozzle to acoustic and entropy disturbances. *J. Sound Vib.* **52**, 283.

FFOWCS WILLIAMS, J. E. & HOWE, M. S. 1975 The generation of sound by density inhomogeneities in low Mach number nozzle flows. *J. Fluid Mech.* **70**, 605.

HOCH, R. & HAWKINS, R. 1973 Recent studies into Concorde noise reduction. *AGARD Conf. Proc.* no. 131, paper 19.

HOWE, M. S. 1975 Contributions to the theory of aerodynamic sound, with application to excess jet noise and the theory of the flute. *J. Fluid Mech.* **71**, 625.

MARBLE, F. E. & CANDEL, S. M. 1977 Acoustic disturbance from gas non-uniformities convected through a nozzle. *J. Sound Vib.* **55**, 225.

SEDNEY, R. 1970 The method of characteristics. In *Nonequilibrium Flows*, part 2 (ed. P. P. Wegener), pp. 160–225. Dekker.

WHITFIELD, O. J. & HOWE, M. S. 1976 The generation of sound by two-phase nozzle flows and its relevance to excess noise of jet engines. *J. Fluid Mech.* **75**, 553.